PROCEEDINGS OF SPIE

SPIEDigitalLibrary.org/conference-proceedings-of-spie

Smoothing mid-spatial frequency (MSF) errors on freeform optics with an algorithm-based robotic platform utilizing deflectometry input

Coniglio, Jennifer, Quattrociocchi, Nick, Eisner, Matthew, Beagley, Starbuck, Beck, Joshua, et al.

Jennifer Coniglio, Nick Quattrociocchi, Matthew Eisner, Starbuck Beagley, Joshua Beck, Daniel R. Brooks, Brittany Cox, Jamie Perdue, Jessica DeGroote Nelson, "Smoothing mid-spatial frequency (MSF) errors on freeform optics with an algorithm-based robotic platform utilizing deflectometry input," Proc. SPIE 11889, Optifab 2021, 118891D (10 December 2021); doi: 10.1117/12.2602729

Event: SPIE Optifab, 2021, Rochester, New York, United States

Downloaded From: https://www.spiedigitallibrary.org/conference-proceedings-of-spie on 31 Jan 2022 Terms of Use: https://www.spiedigitallibrary.org/terms-of-use

Smoothing Mid-Spatial Frequency (MSF) Errors on Freeform Optics with an Algorithm-based Robotic Platform Utilizing Deflectometry Input

Jennifer Coniglio*[a], Nicholas Quattrociocchi, Matthew Eisner, Starbuck Beagley, Josh Beck, Daniel R. Brooks, Brittany Cox, Jamie Perdue, Jessica DeGroote Nelson
[a] Optimax Systems, Inc., 6367 Dean Parkway, Ontario, NY USA 14529-8939

ABSTRACT

Freeform optics offer great flexibility in design parameters, but the subaperture techniques required for manufacture often result in mid-spatial frequency (MSF) errors that can impact final performance. These errors must be removed, but the options to do so, often requiring hand-smoothing by a skilled artisan, are costly and time-consuming. Optimax has developed the HERMES (High End Robotic MSF Elimination System) a robotic platform that uses a machine learning algorithm to smooth parts. Preliminary research indicated promising results, but the process had not yet been compared to the "gold standard" of human smoothing. Results indicate that HERMES fared well compared to smoothing results of a highly skilled artisan. Future directions for work are discussed.

Keywords: MSF Errors, optics manufacturing, freeform optics

1. INTRODUCTION

The optics industry is seeking more and more precise and sophisticated lenses for a variety of purposes. Optical designers are incorporating freeform optics to expand flexibility in the shape, size, and weight components. The versatility in designs offered by freeforms can help reduce optical system size and areal density. Freeform optics can offer powerful solutions for applications such as telescopes, heads up displays, augmented and virtual reality, compact imaging, and more.

Full-aperture polishing on freeform optics, defined as including surfaces lacking axial or radial symmetry, is not possible because of the change of curvature of the surface. Instead, they are fabricated via sub-aperture or single point form generation and polishing. Sub-aperture polishing is typically composed of a rotating compliant tool and active layer, which follows the prescribed change in curvature of the optic as it is pressed into the optic's surface to create a polishing spot. The Computer Numerical Controlled (CNC) tool-path is commanded via software, and can be executed across multiple platforms, including a robotic arm. In dwell-based correction, the tool moves across the part and surface speed is adjusted to correct form and surface errors. However, these techniques can induce mid-spatial frequency (MSF) errors into the optical surfaces (Figure 1), and although there are some techniques to help prevent some MSF errors from forming, surfaces are frequently left with errors requiring smoothing.

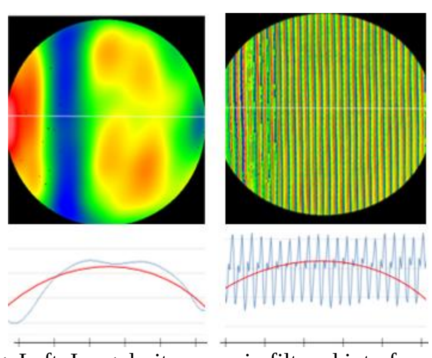

Figure 1: Errors in optic manufacturing. Left, Irregularity error, in filtered interferometry data, showing low order error of a part. Right, MSF error from the same part, filtered to show errors in this regime. These errors were induced from raster polishing with a robotic platform.

*jconiglio@optimaxsi.com; Phone: 1.585.265.1020; optimaxsi.com

Optifab 2021, edited by Jessica DeGroote Nelson, Blair L. Unger, Proc. of SPIE
Vol. 11889, 118891D · © 2021 SPIE · 0277-786X · doi: 10.1117/12.2602729

Downloaded From: https://www.spiedigitallibrary.org/conference-proceedings-of-spie on 31 Jan 2022
Terms of Use: https://www.spiedigitallibrary.org/terms-of-use

MSF errors can appear at spatial frequencies of 0.01 mm^{-1} to 10s of mm^{-1}, and are distinct from surface roughness[1]. However, there are not strict frequency limits; the size range of MSF error is defined by the optical systems requirements and the manufacturing technique chosen. MSF errors degrade image quality and the point spread function of optics and systems. In directed energy applications, the resulting small angle scatter can cause catastrophic hot spots. MSF errors must be eliminated to achieve diffraction-limited ultra violet (UV) and visible (VIS) image quality, which is simulated in (Figure 2). MSF errors can be visualized and described via power spectral density (PSD) plots[2]. Briefly, PSD plots describe the amplitude of a surface in relation to frequency[3]. PSD plots are based on Fast Fourier transformations of sampling of the optical surface, which allows investigation into the dominant frequencies of errors across the band of interest (Figure 3).

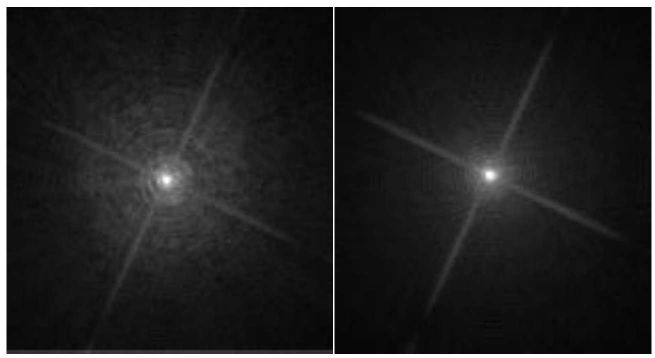

Figure 2: (Left) Simulated point spread function (PSF) plot degraded due to MSF. (Right) PSF without MSF error impact. [Adapted from Hull, et al.[2]].

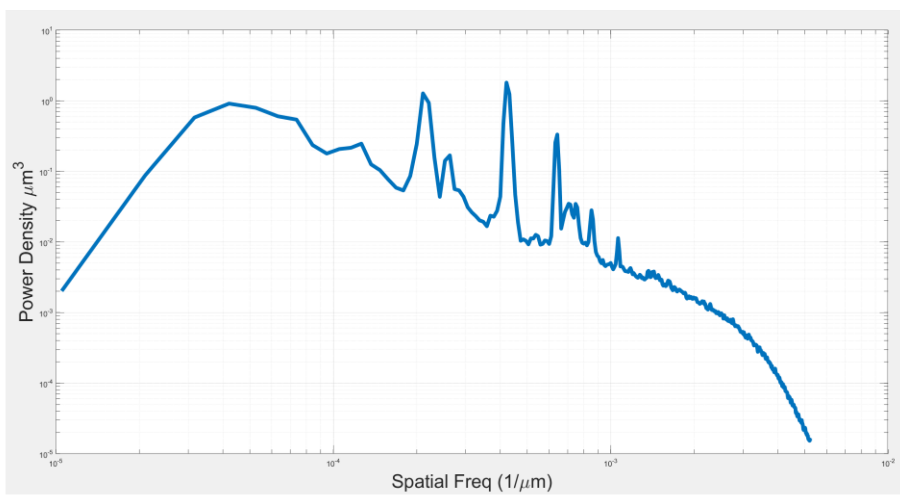

Figure 3: Power Spectral Density (PSD) plot of an optical surface showing a significant signature at about 0.42 mm^{-1}.

Correction of MSF errors is necessary but only limited techniques exist, and these methods are costly and time consuming. These errors are still frequently mitigated via hand smoothing completed by highly skilled master opticians[1]. The process is time consuming, tedious, and physically demanding on individuals and they are unable to attend to other value-added work. Other MSF error reduction techniques have been studied as well, including use of VIBE technology[4], specialized polishing apparatus[5], and more. Regardless of the MSF error smoothing methodology, there remains a balance between MSF error correction and resulting loss of form, requiring an iterative loop (Figure 4).

Downloaded From: https://www.spiedigitallibrary.org/conference-proceedings-of-spie on 31 Jan 2022
Terms of Use: https://www.spiedigitallibrary.org/terms-of-use

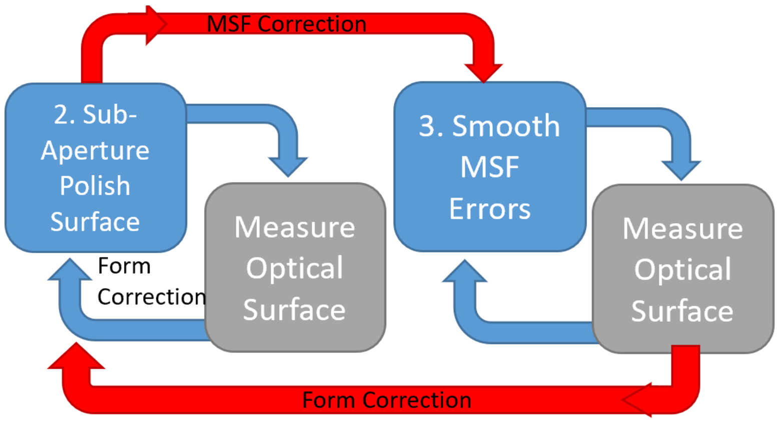

Figure 4: MSF error correction occurs after subaperture polishing, but results in inherent loss of form. Typically, the process then stops MSF smoothing and returns to form correction, and the loop continues until specified criteria are met.

2. DEVELOPMENT OF HERMES

Optimax has been exploring the use of collaborative robots (Cobots) to automate the hand-smoothing process in an effort to reduce cost, turn-around time, and free up artisans for other value-added work. As part of the HERMES (High End Robotic MSF Elimination System), the hand smoothing technique employed by a human was studied to help develop a machine-learning algorithm for robotic smoothing. The development of the algorithm starts with metrology data of the part that needs smoothing, a smoothing path recorded from tracking the technique employed by the artisan, and the measurement of the part after smoothing. All three of these are processed by the algorithm which then returns a toolpath and time prediction to for MSF smoothing as shown in Figure 5.

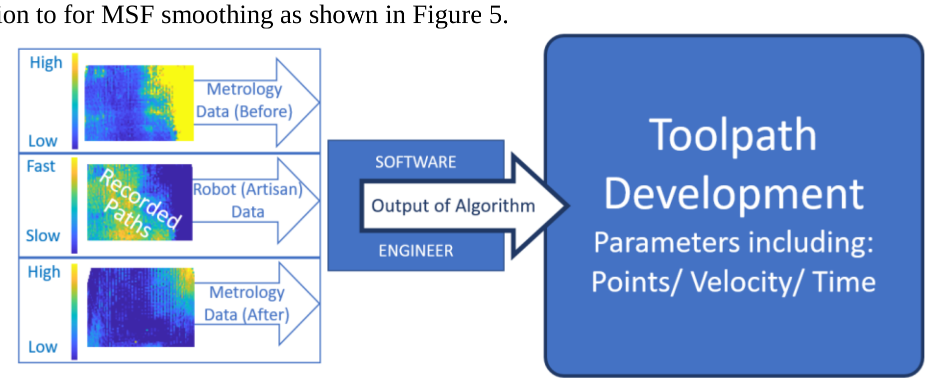

Figure 5: HERMES concept: Deflectometry metrology data is entered into an algorithm, which then outputs a toolpath and time prediction for MSF smoothing.

First, to test the smoothing of a robot arm, an artisan smoothing technique that consistently resulted in smoothed surfaces was studied. Fused silica sample parts were polished with another robotic platform with a path that intentionally resulted in MSF errors at a frequency commensurate with the path parameters. That is, the errors were generated at a frequency set by the robotic path (e.g., between one and 5 mm between passes) in one direction (e.g., all in the X direction). These errors were measured using deflectometry techniques and analyzed using PSD data that were determined, based on Zygo's Mx software[6] (Figure 6). Specialized tooling was developed and artisan 'hand smoothing' paths were recorded, and repeated on the collaborative robot until MSF errors were lessened (Figure 7). The part was smoothed with the recorded path until the MSF error had decreased according to the PSD data (Figure 8). This portion of the project acted as the "inspiration" for the remaining work.

Downloaded From: https://www.spiedigitallibrary.org/conference-proceedings-of-spie on 31 Jan 2022
Terms of Use: https://www.spiedigitallibrary.org/terms-of-use

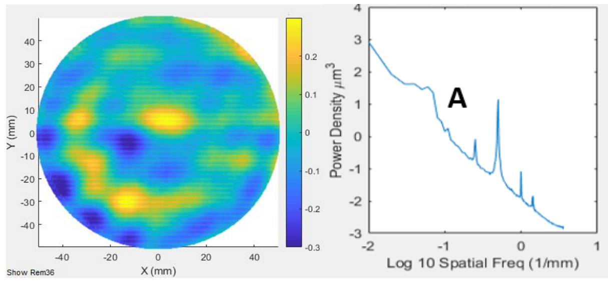

Figure 6: Left, deflectometry representation of a fused silica part with robot raster lines present. Right, Power Spectral Density analysis of the same part. Data were collected via deflectometry and then entered into Mx for PSD analysis.

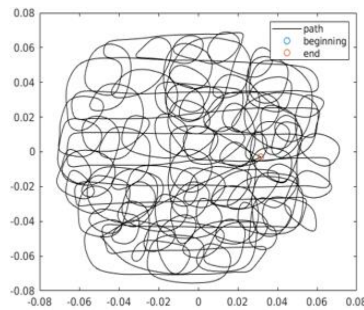

Figure 7: Artisan hand-smoothing path recorded on the collaborative robot (Cobot) for initial program development.

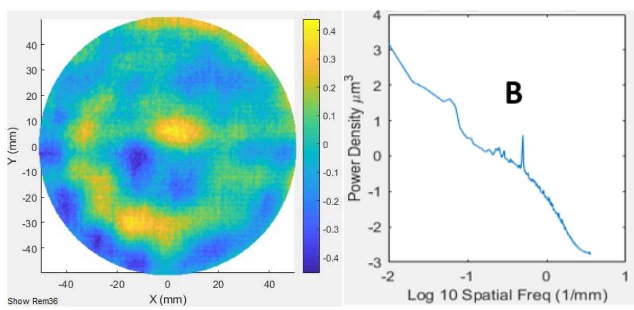

Figure 8: Post cobot applied recorded artisan path (repeated) showing reduction in PSD from deflectometry data.

Once it was clear that the robot could smooth, work was done to create toolpaths generated by the algorithm that would accomplish similar results. Much effort was devoted to creating paths that would emulate the human-recorded path, and a trochoidal path was eventually adopted (Figure 9). This path, based on artisan input, was developed to provide uniform coverage of the part, and the current algorithm allows the paths to be projected onto virtually any surface using several six-axis in-house robots.

Downloaded From: https://www.spiedigitallibrary.org/conference-proceedings-of-spie on 31 Jan 2022
Terms of Use: https://www.spiedigitallibrary.org/terms-of-use

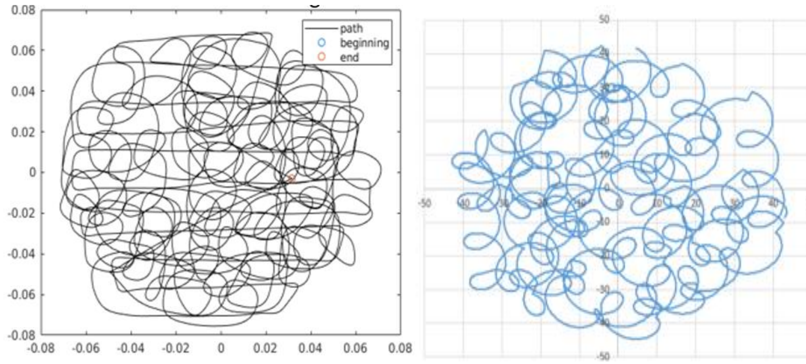

Figure 9: Left, an artisan-recorded path illustrating the circular motion of the smoothing path. Right, a Trochoidal version of the HERMES path repeated for initial smoothing runs.

A "go-no go" criteria for sufficient PSD amplitude reduction was utilized for the project as the algorithm required an easily quantified criterion. Because the MSF errors were unidirectional from the robot rastering, a PSD Ratio was developed. As noted above, the data collection optics were robot raster polished and there was a definitive lay and frequency of MSF errors. This metric consisted of the PSD RMS for the targeted frequencies in the X direction (Average X) versus the Y direction (Average Y) as these measurements were "against the lay" of the MSF errors. It was deemed that if the errors in the targeted direction neared the errors in the orthogonal direction, the ratio of the RMS under the PSD curve would approach one. This ratio was calculated according to Equation 1, and was used as a metric for later work.

$$PSD\ Ratio = \frac{PSD\ RMS\ Direction\ 1}{PSD\ RMS\ \ Direction\ 2} \tag{1}$$

2.1 Initial Results of HERMES.

Initial HERMES tests indicated good MSF error reduction per the PSD ratio criteria (e.g., Figure 10, Figure 11). Preliminary data for the project suggested that the HERMES algorithm could smooth parts that took anywhere from 6 to 26 hours, time that could free up artisans for other tasks.

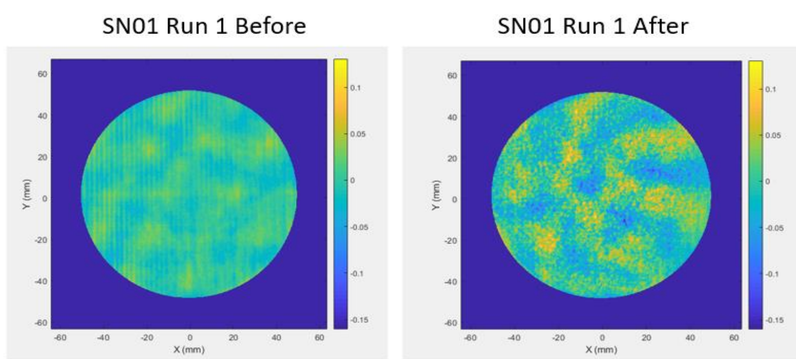

Figure 10: HERMES deflectometry images of a part before (left) and after (right) smoothing with the HERMES tool path.

Downloaded From: https://www.spiedigitallibrary.org/conference-proceedings-of-spie on 31 Jan 2022
Terms of Use: https://www.spiedigitallibrary.org/terms-of-use

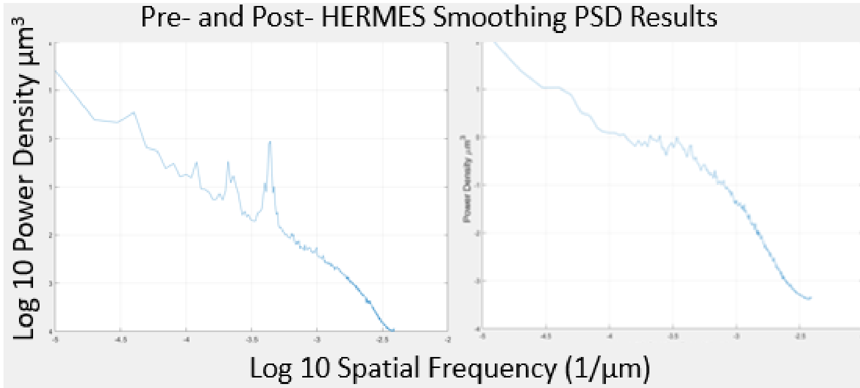

Figure 11: Early HERMES smoothing test on one part showing before (left) and after (right) PSD for single direction average PSD.

2.2 Smoothing Criterion and Algorithm Development.

Several issues were noted during the early HERMES development. First, it was noted that a decrease in the PSD peak was accompanied by other changes in the form of the part. This phenomenon is expected when the part is smoothed, even when it is hand-smoothed. The overall RMS of the part was not initially considered in the deflectometry data as these data do not capture form error well. To help address this concern, the algorithm was adapted to include RMS data from interferometry files to represent change in desired form. For later HERMES runs, the RMS data were monitored along with the PSD ratio, and the change in each was predicted based on data collected (Figure 12). Based on these data, the smoothing runtime can now be predicted to optimize the change in PSD ratio against the loss of form (RMS). Additional trials will be needed to refine this prediction.

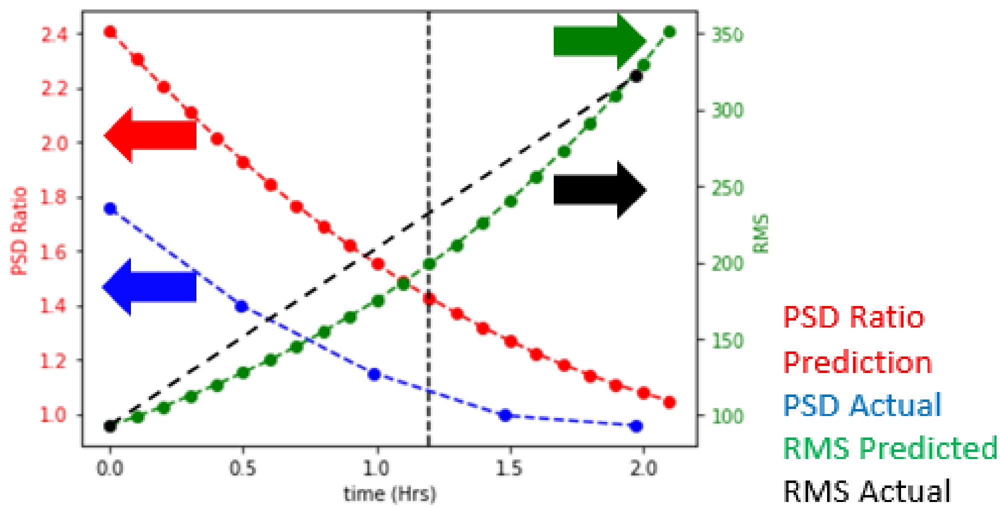

Figure 12: Algorithm prediction refinement for an example HERMES run. Red line represents Predicted PSD Ratio reduction (from deflectometry data); Blue line represents the actual PSD ratio reduction; Green line is the predicted change in RMS (interferometry data), and black line is actual RMS change (nm). To balance the MSF improvement with the RMS degradation, the algorithm predicts an "optimal" stopping point (black vertical line).

Secondly, the PSD ratio described above, although helpful for initial "go-no go" decisions of an algorithm, is not a representative metric for monitoring MSF change. This is because as both directions, even those orthogonal, would increase in error through the smoothing process, and therefore the ratio would decrease without meaningful improvement in optical surface quality. Optimax is currently working on improving the MSF error quantification for the algorithm input.

Downloaded From: https://www.spiedigitallibrary.org/conference-proceedings-of-spie on 31 Jan 2022
Terms of Use: https://www.spiedigitallibrary.org/terms-of-use

3. HERMES VS. HAND SMOOTHING

3.1 Direct Comparison

Finally, there was no direct comparison of HERMES smoothing to the existing standard process of hand smoothing an optic. For the current project, a head-to-head comparison was arranged, such that the current form of HERMES could be compared against the industry standard technique. The results will be used to further refine the HERMES algorithm.

For this phase, the goal was to compare the results of smoothing two similar optics, one with HERMES and one by a skilled artisan. Instead of running the computer toolpath based on the algorithm predictions, the path was repeated for a total smoothing time comparable to the hand-smoothed part to better directly compare the results over time of HERMES compared to hand smoothing and because of the “go-no go” criteria is still evolving.

Two fused silica parts, with approximately 95 mm diameter clear aperture, and a long concave radius were raster polished using the same robotic platform. Parts were measured with interferometry (Figure 13) and deflectometry (Figure 14) before and at regular intervals during the competition. Zygo’s Mx software[6] PSD algorithm for Non-Directional PSD was used for the comparison.

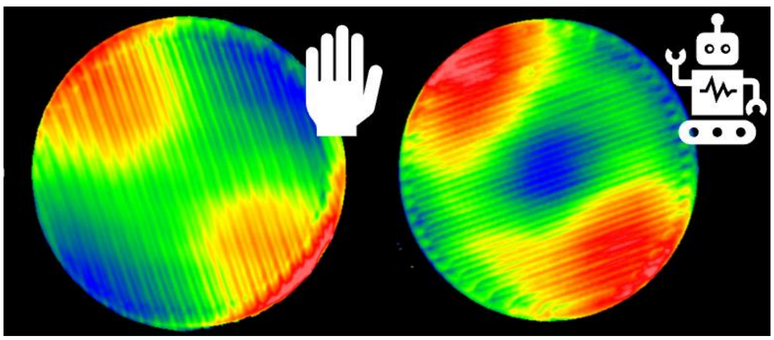

Figure 13: Initial interferometry data for the two "Bake Off" Parts. Left was the part used on the HERMES platform (RMS 0.048 µm), Right was the hand-smoothed part (0.062 µm).

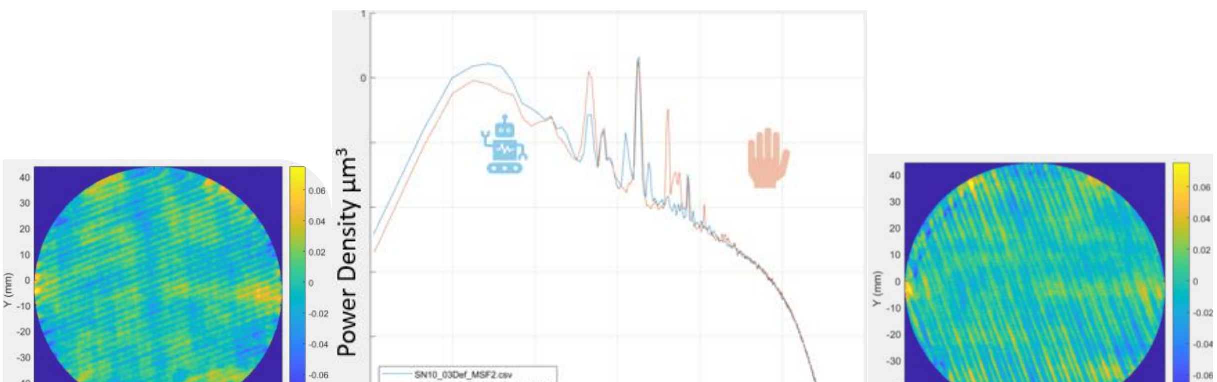

Figure 14: Initial deflectometry data for the two comparison parts. Left, the HERMES part; Center, the PSD data for each part, robot (blue) and hand smoothed (orange); Right, the hand smoothed part. The Peak PSD amplitude value (HERMES: 2.08 µm^3, HAND: 1.80 µm^3) was monitored for this project.

Rules for the “competition” were as follows: For the Hand Smoothed part, no rotation of the part was allowed, but the artisan was allowed to select his active layer and pad size. However, the slurry was the same as what was used on the HERMES part. The hand smoothing sessions were 10 minutes each. For the HERMES part, the setup of the robot was the same as on other HERMES runs, including repeating an evenly distributed, randomized path (but without time prediction),

Downloaded From: https://www.spiedigitallibrary.org/conference-proceedings-of-spie on 31 Jan 2022
Terms of Use: https://www.spiedigitallibrary.org/terms-of-use

pad size, slurry, etc. were the same as on other trials, with the exception of the last few runs where the setup was matched to the active layer chosen by the artisan. Per previous HERMES runs, the force was held constant throughout the runs.

3.2 Pre- and Post- Results.

The data for about 275 minutes of HERMES runs were compared to 260 Hand smoothing minutes on the parts. Deflectometry data were monitored in two ways: the peak PSD amplitude value was monitored for each run, as well as the overall PSD curve. These data were collected for nearly every run. In addition, the interferometry RMS data were collected after sets of several runs for each part. Figure 15 shows the progress of the HERMES vs. the hand smoothed parts over subsequent runs. Both parts showed similar decreases in peak PSD amplitude (55.4% reduction for the HERMES part and 67.8% reduction for the Hand Smoothed part). It should be noted that the PSD amplitude of the Hand Smoothed part started and ended somewhat lower than the HERMES part. Both parts showed a plateau towards the end of the process, and the HERMES smoothing was continued to 398 minutes to test limits (not shown), but without further improvement in the peak PSD. While the HERMES part showed a fairly linear increase in RMS error, the hand smoothed part was more "stepwise" in its increase.

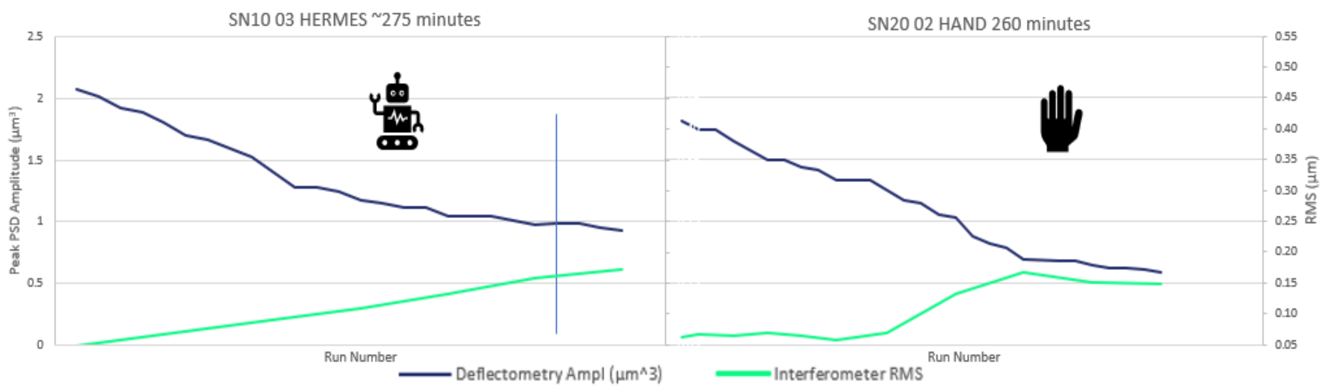

Figure 15: Peak PSD amplitude (blue) and RMS (green) over time for the HERMES (Left) and hand smoothed (Right) parts. Both parts show a similar decrease over time in Peak PSD amplitude, with the hand smoothed part plateauing with slightly better performance than the HERMES part. The RMS loss was linear for the HERMES part, but more "stepwise" for the hand smoothed part.

Deflectometry data before and after smoothing is compared in Figure 16 and Figure 17. While both the hand smoothing and the HERMES smoothing provided some increase in overall error as noted in the PSD curves, the change in the HERMES part was somewhat greater across the bands of interest. While the HERMES part broke up the prominent PSD peak, it did create slightly greater changes in other frequencies.

Downloaded From: https://www.spiedigitallibrary.org/conference-proceedings-of-spie on 31 Jan 2022
Terms of Use: https://www.spiedigitallibrary.org/terms-of-use

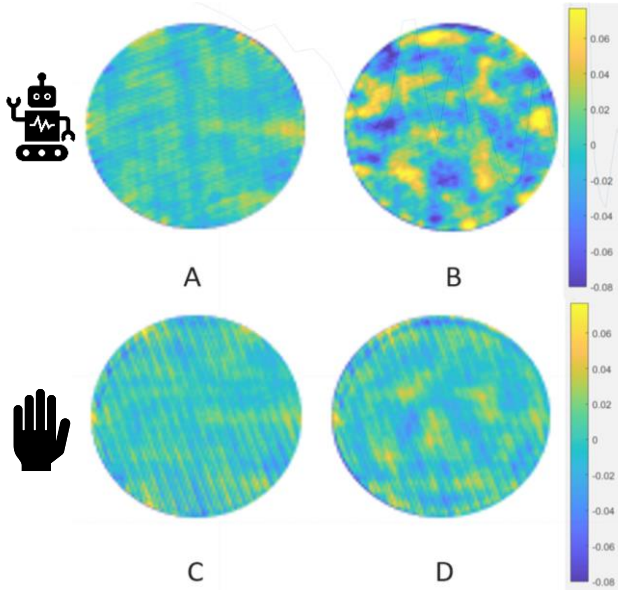

Figure 16: A and B are pre and Post deflectometry images of the HERMES smoothed part, and C and D are pre and post images of the Hand smoothed part (scale in µm).

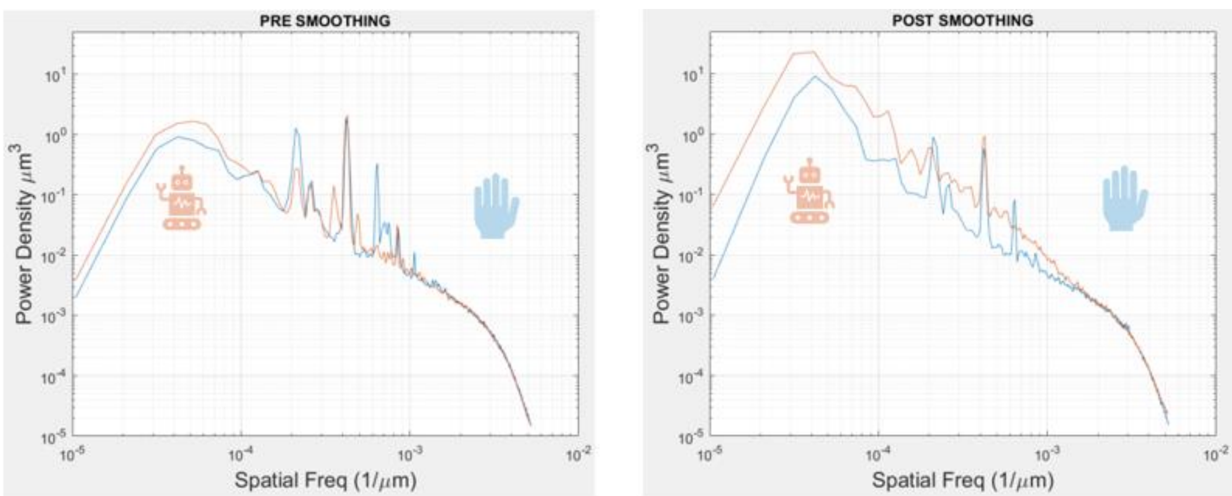

Figure 17: Pre and Post Deflectometry PSD curves for the HERMES and Hand-Smoothed parts for the 260 minutes of Hand smoothing and 275 minutes of HERMES smoothing. Both parts showed a reduction in the peak PSD amplitude and an increase in amplitudes in lower order error. The HERMES part did show a greater increase in the amplitude other MSF frequency ranges, but succeeded in breaking up the strongest PSD frequency signatures.

3.3 Future Work.

As noted, the RMS for the HERMES part showed a fairly linear progression, which was different than that of the hand smoothed part. Discussion with the artisan during the process suggests that feedback from interferometry data was incorporated to "fix" errors that began to appear. That is, the artisan looks to "hit" high spots with more force to help reduce error and return the form to the desired shape (Figure 18). This observation has been noted previously, and is something that can be applied directly to the HERMES smoothing algorithm.

Downloaded From: https://www.spiedigitallibrary.org/conference-proceedings-of-spie on 31 Jan 2022
Terms of Use: https://www.spiedigitallibrary.org/terms-of-use

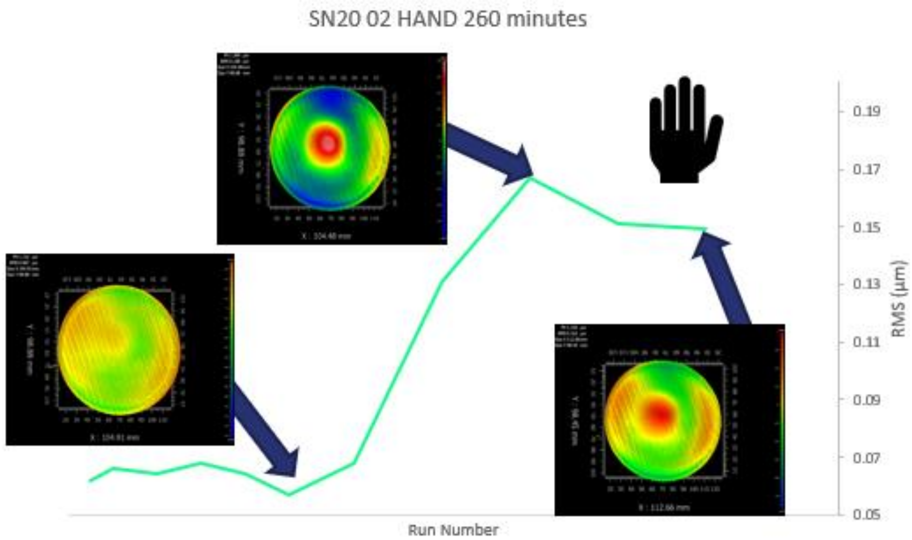

Figure 18: Overview of the Hand-Smoothed change in RMS. the change was not linear as compared to the HERMES change, and the artisan noted "targeted" smoothing to address the "high spot" seen in the center of the part (interferometry data). This selective smoothing allowed the artisan to simultaneously address MSF and form error.

In its current structure, HERMES paths are randomly generated and then repeated until the part reaches a more smoothed state. One potential area of improvement would be to provide variations in the smoothing toolpaths, to help reduce the chances that a path would generate its own signature. To help address the vast need for data for the machine learning algorithm, the current data collection methods for the HERMES project rely on multiple short paths with data in between, but this same approach could be improved by creating subsequent paths based on data.

Another project, Force Controlled HERMES (FC HERMES) recently showed that a programmed toolpath can incorporate a specific force range as dictated by location on the part. For that project, the underlying structures of a light-weighted part were identified and used to create a gradient of forces applied while smoothing (Figure 19). The same toolpath development software can be utilized to address changes in form as smoothing occurs, to target, just as is done during hand smoothing. Interferometry data can be mapped to locations on the parts surface, and used to create a "force gradient" to apply during the smoothing process. This addition would help refine the MSF error correction process to include Force Form Correction during the smoothing cycle, and potentially further refine the HERMES smoothing process and algorithm.

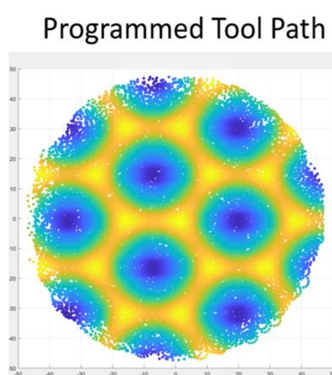

Figure 19: An FC HERMES toolpath showing changes in smoothing force as dictated by location on a part. In this case, the forces were determined based upon properties of the part (geometry of face sheet thickness of a light-weighted optic). The same methodology can be used to incorporate interferometry data to target form error with gradient force in HERMES smoothing paths.

The forces used by the artisan for the entirety of the part are not yet well documented and may be an additional area of ongoing investigation. Previous artisan recordings did not include sufficient force data due to deficits in the cobot

Downloaded From: https://www.spiedigitallibrary.org/conference-proceedings-of-spie on 31 Jan 2022
Terms of Use: https://www.spiedigitallibrary.org/terms-of-use

programming. Additional information on the forces used by the artisan to smooth can help further refine the HERMES algorithm to define the Force Form Correction force gradient to apply to parts.

4. SUMMARY

The HERMES smoothing process and algorithm performed well compared to a hand smoothing "competitor", in terms of PSD changes where both parts showed decreases in peak PSD amplitude of more than 55%. Additional factors, including form error correction, are opportunities for further work. Ongoing data collection will help refine the algorithm time predictions to increase automation.

REFERENCES

[1] Tinker, F.; Xin, K., "Correlation of mid-spatial features to image performance in aspheric optics," Proc. SPIE 8837, Material Technologies and Applications to Optics, Structures, Components, and Sub-Systems, p. doi: 10.1117/12.2028015, 30 September 2013.

[2] Hull, T., Riso, M. J., Barentine, J. M., & Magruder, A. , "Mid-spatial frequency matters: examples of the control of the power spectral density and what that means to the performance of imaging systems," Proc. SPIE 8353, Infrared Technology and Applications XXXVIII, vol. 835329, 31 May 2012.

[3] Youngworth, R., Gallagher, B., & Stamper, B., "An overview of power spectral density (PSD) calculations," Proc. SPIE 5869: Optics and Photonics, San Diego, California, United States, 2005, DOI:10.1117/12.618478.

[4] Nelson, et. al., "IBE finishing to remove mid-spatial frequency ripple," in International Optical Design Conference and Optical Fabrication and Testing 2010, Jackson Hole, WY. , 2010.

[5] Kim, D. W., & Burge, J. H., "Rigid conformal polishing tool using a non-linear visco-elastic effect," Optics Express, vol. 18, no. 3, pp. 2242-2257, 2010.

[6] Zygo Corporation, Mx Reference Guide OMP-0550C, Middlefield, CT, 2018.

Downloaded From: https://www.spiedigitallibrary.org/conference-proceedings-of-spie on 31 Jan 2022
Terms of Use: https://www.spiedigitallibrary.org/terms-of-use